Title
Performance Evaluation Of Reflective Coatings On Rooftop Units

Author
Design & Engineering Services, Southern California Edison

Publication Date
2004-04-01

PERFORMANCE EVALUATION OF REFLECTIVE COATINGS ON ROOFTOP UNITS

Report on Task I: Analytical Study

DRAFT

Prepared for:
California Energy Commission
1516 9th Street
Sacramento, CA 95814

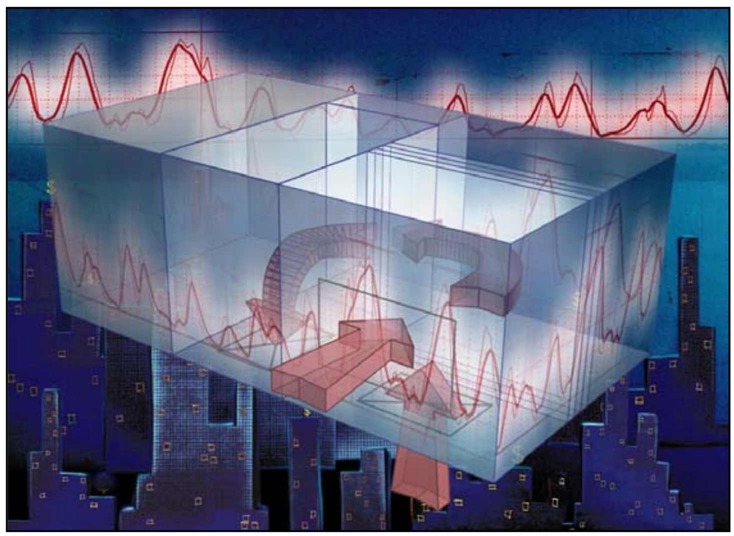

Prepared by:
Design & Engineering Services
Southern California Edison
Irwindale Avenue. Suite B
Irwindale, CA 91702

SOUTHERN CALIFORNIA
EDISON
An *EDISON INTERNATIONAL*℠ Company

April 2004

PERFORMANCE EVALUATION OF REFLECTIVE COATINGS ON ROOFTOP UNITS

Report on Task I: Analytical Study

DRAFT

SUMMARY

A thermal analysis was conducted on a typical 5-ton rooftop air-conditioner to determine the effects on the supply air temperature and cooling performance by adding a highly reflective coating material to its external surfaces. The analysis considered several emissivity values. Under typical conditions, low emissivity (highly reflective) surfaces produced a reduction in the supply air temperature of 0.21°F when compared to high emissivity (low reflectivity) surfaces. In addition, the mixed air temperature was reduced by 0.07°F when a low emissivity (ε = 0.2) surface was considered. The result of this reduced mixed air temperature is a lower coil-entering air temperature, which, in turn, produced an increase of 0.29 percent in the cooling capacity of the unit.

BACKGROUND

A large percentage of HVAC equipment used in California's small commercial sector consists of packaged rooftop air conditioners with capacities between 5 and 10 tons. One of the most common units within this capacity range is a 5-ton rooftop unit (RTU) that can be found in both residential and small commercial applications. These units are typically mounted on building roofs and are exposed to intense direct and indirect solar radiation. Solar radiation increases the exterior surface temperature of the evaporator compartment of the RTU and causes heat to flow from the cabinet into the supply air stream. It is expected that lower surface temperatures would result by applying a highly reflective coating (HRC) material to the exterior of the RTU cabinet.

The objective of this investigation is to determine the impact of a HRC material on the supply air temperature and cooling performance of RTUs. This investigation has four tasks:

Task I: Analytical Study
Task II: Preliminary Field Testing
Task III: Experimental
Task IV: Field Monitoring

This report addresses the results of Task I: Analytical Study.

METHODOLOGY

A thermal analysis was conducted on a typical 5-ton RTU to determine the effects on the supply air temperature and cooling performance of the RTU by adding a HRC material to the external surfaces. A Lennox L Series gas/electric RTU was used for the analysis. Figure 1 provides general dimensions and multiple views of the 5-ton Lennox unit (model number 060).

The RTU thermal analysis was divided into seven main parts:
1. Key Variables
2. Key Assumptions
3. RTU Model Description
4. RTU Conductive, Convective, and Radiative Fluxes Characterization
5. Solar Radiation
6. Wind Speed
7. Parametric Runs and Typical Condition

KEY VARIABLES

The analysis took into account the solar absorptivity (α) and reflectivity (ρ) of the RTU exterior surfaces and the infrared emissivity (ε) of the RTU exterior and interior surfaces, where $\alpha = (1- \rho)$ and $\varepsilon = \alpha$.

The solar radiation, atmospheric temperature, wind speed, and RTU cabinet insulation thickness were key variables in the analysis. Other important variables were: supply air temperature leaving the RTU, mix air temperature, cooling coil surface temperature, coil-leaving air temperature, return air temperature, thickness of RTU exterior wall, thickness of insulation, and the infrared surface emissivities of the cooling coils and the air filter.

KEY ASSUMPTIONS

The absorptivity, reflectivity, and emissivity of the RTU surfaces had no angular or spectral (wavelength) dependencies. In other words, they were considered total hemispherical properties.

The emissivity of the cooling coil was assumed to be 0.1. The emissivity for the RTU interior surfaces was assumed to 1.0 (surfaces covered with dust).

The analysis assumed a constant cooling coil surface temperature of 45°F and a constant coil leaving air temperature of 56°F. These values were based on laboratory tests performed at the Southern California Edison's Refrigeration and Thermal Test Center on a 5-ton RTU for the "Performance Evaluation of 5-ton RTU under High Ambient Temperature" project. These temperatures were obtained for an ambient temperature of 85°F, which was also the ambient temperature used in the analysis.

DIMENSIONS AND WEIGHTS - INCHES (MM)

Shown With Economizer Dampers, Power Exhaust Fan, Convenience Outlet, Disconnect, Belt Drive Blower

Model No.	WEIGHTS				CORNER WEIGHTS - Base Unit								CENTER OF GRAVITY			
	Net		Shipping		AA		BB		CC		DD		EE		FF	
	lbs.	kg	lbs.	kg	lbs.	kg	lbs.	kg	lbs.	kg	lbs.	kg	in.	mm	in.	mm
036	656	298	786	357	120	54	146	66	215	98	176	80	18-3/4	476	39-3/8	1000
042	656	298	786	357	120	54	146	66	215	98	176	80	18-3/4	476	39-3/8	1000
048	720	327	850	386	146	66	158	72	227	103	209	95	19	483	42	1067
060	730	331	860	390	146	66	160	73	233	106	211	96	18-7/8	479	41-5/8	1057
072S	745	338	875	397	161	73	174	79	228	104	212	96	20-1/8	511	42-1/8	1070
072H	755	342	885	401	161	73	174	79	228	104	212	96	20-1/8	511	42-1/8	1070

ACCESSORY SHIPPING WEIGHTS (add to base unit weight)

Dual/High Fire Heat Exchanger	18 lbs	8 kg	LTL Packaging (less than truck load)	8 lbs.	4 kg
Economizer + Hood	52 lbs.	24 kg	Barometric Relief Damper	15 lbs.	7 kg
Outdoor Air Damper + Hood	64 lbs.	29 kg	Hood for Barometric Relief Damper	13 lbs.	6 kg

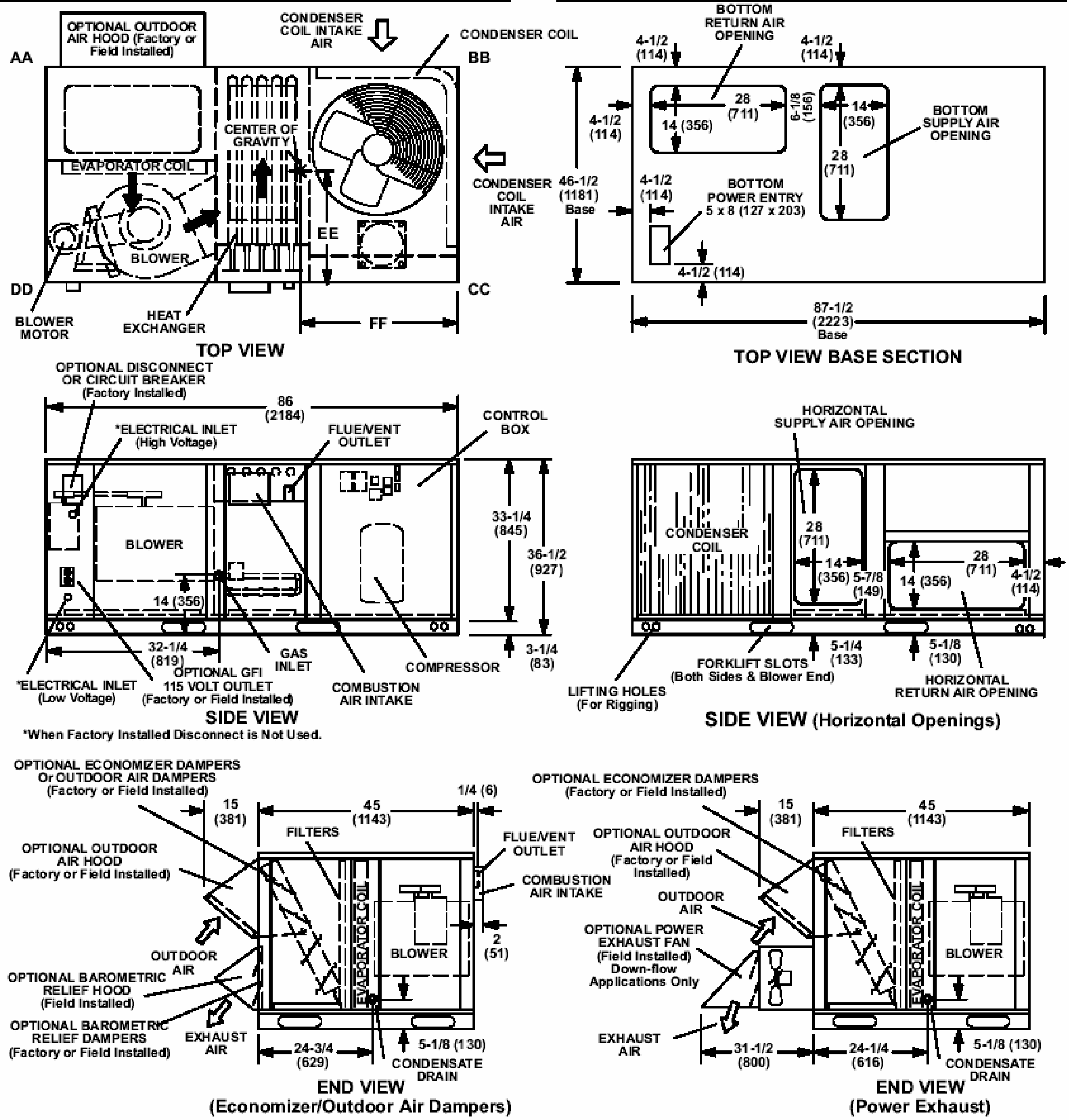

Figure 1: Dimensions and Views of Lennox L Series 3- to 6-ton RTU

The return air temperature was assumed to be 79°F, and the outside air fraction was fixed at 15 percent. In addition, the thermal proprieties of air were assumed to be constant over the expected range of temperatures in the analysis.

The blower motor heat and any moisture in the air were not considered in the analysis. The motor heat was neglected because it is a constant regardless if the external surface of the unit has a highly reflective coating or not, and its impact on the evaluation of the benefits of highly reflective coating was considered minor.

The moisture in the air was not considered because of the added complexity in the heat transfer calculations. In the case of the convective fluxes not only heat, but also mass transfer would have to be considered. In the case of radiative fluxes, the spectral (wavelength) dependencies would have to be introduced. As it was with the case of the blower motor heat, the impact of moisture was considered minor for the purpose of evaluating the benefits of highly reflective coatings on the external surfaces of the RTU. Therefore, only sensible heat was considered.

In the analysis, the convective heat transfer coefficients were calculated using a Nusselt number correlation for turbulent flow over a flat plate. This is a reasonable assumption when considering the air flow path and geometry of the various sections in the RTU. Also to account for the air path complexity of the section where the blower and motor assembly are, the air velocity was double.

The heat transfer by conduction thru the RTU metal surfaces and insulation was assumed to be steady-state, one-dimensional and perpendicular to the surfaces. The insulation was assumed to be fiberglass with a thermal conductivity of 0.031 Btu/hr-ft-°F. The conductive heat fluxes were calculated using the Fourier's Law.

RTU MODEL DESCRIPTION

The RTU was divided into five main sections: (1) Mix Air Section, (2) Cooling Section, (3) Heating Section, (4) Combustion Air Intake Section, and (5) Condenser Section, of which the first three sections, where the conditioned air flows, were considered for the modeling of the unit. The model did not account for a possible outside air hood in the Mix Air Section. Figures 2a and 2b show the location, relationship, and orientation of each of the sections in the model as well as the air flow path.

The unit exterior top and side surfaces absorb direct and diffuse solar radiation, emit thermal radiation, and convectively interact with the atmospheric air. The exterior bottom surface, although not in direct contact with the roof, was considered adiabatic. The interior surface separating the Heating Section from the Condenser Section was also considered adiabatic. In addition, the west surface of the Heating Section was considered adiabatic as the Combustion Air Intake chamber separates it from the exterior surface (see Figures 2a and 2b). The analysis allows for interior surfaces with

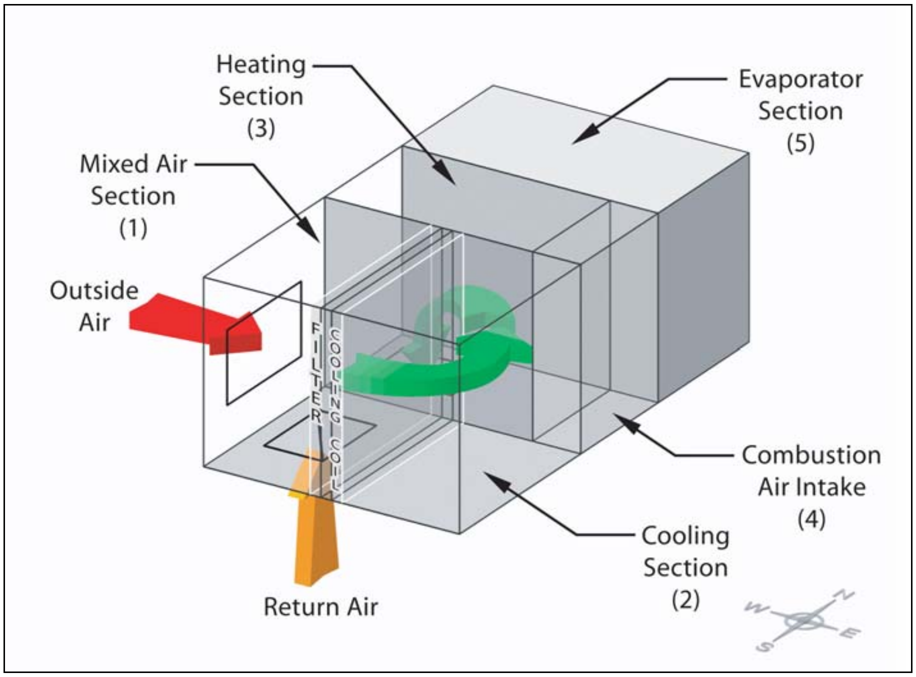

Figure 2a: RTU Model Sections, Orientation and Air Flow Path – East View

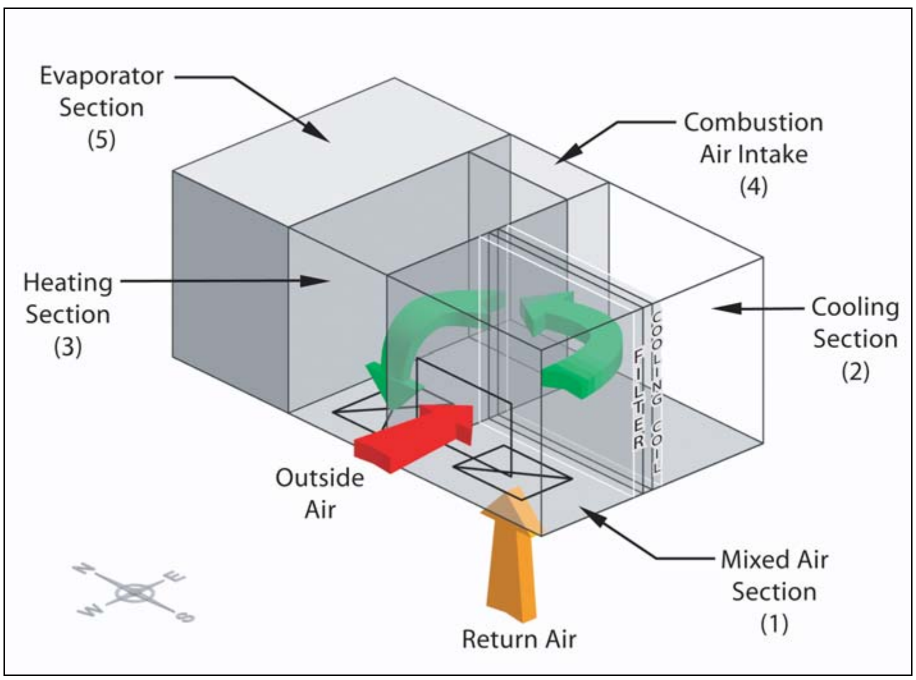

Figure 2b: RTU Model Sections, Orientation and Air Flow Path – West View

or without insulation. Within each section, the surfaces interact radiatively with each other and convectively with the conditioned (or mixed) air.

RTU Conductive, Convective and Radiative Fluxes Characterization

A steady-state energy balance was conducted on each surface, with an unknown temperature, and the air, generating a set of equations. The conduction through the exterior walls was considered in terms of a thermal resistance being the sum of the thermal resistances for the metal walls and the insulation. The convective fluxes were parameterized using Newton's law of cooling. The heat transfer coefficient was obtained using a Nusselt number correlation for turbulent flow over a flat plate, where the Nusselt number is a function of Reynolds and Prandtl numbers. The radiative fluxes were calculated by calculating shape factors and using input emissivities along with the Stefan-Boltzmann law for blackbody emission. Figure 3 shows a representation of the various heat transfer modes thru a simple resistance network.

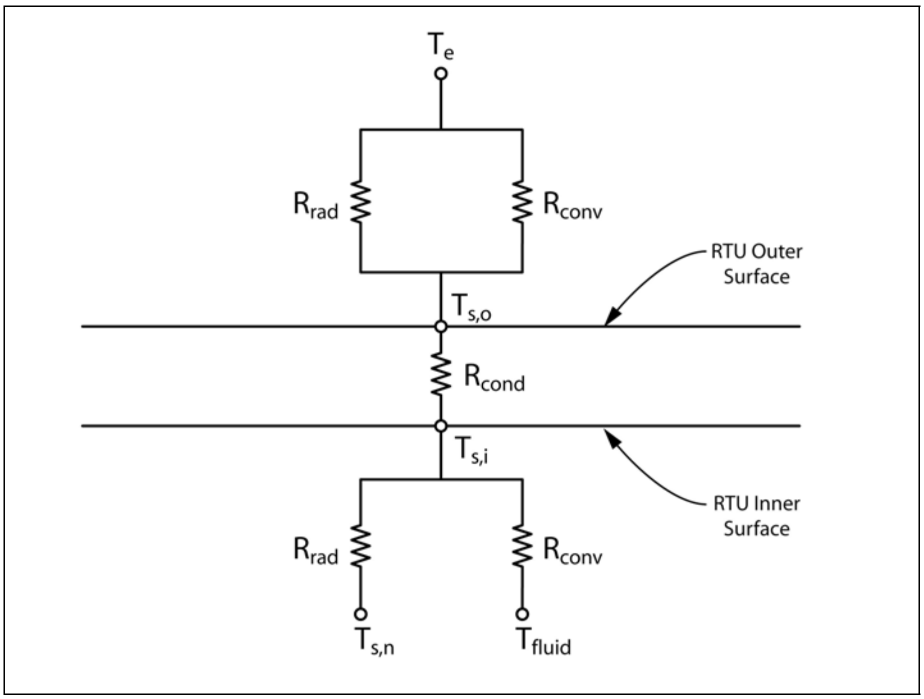

Figure 3: Heat Transfer Resistance Network

In Figure 3, R_{rad}, R_{conv}, R_{cond} represent the resistances associated with the radiation, convection, and conduction heat flows. T_e represents an effective surrounding temperature. $T_{s,n}$ represents the various inner surfaces temperatures, while T_{fluid} represents the temperature of the conditioned or mixed air within the RU.

The system of equations to be solved is nonlinear and must be solved iteratively. The approach was to solve a linear system of equations where the conductive and convective heat flows were represented in terms of the temperatures. Then, for that set of temperatures the radiative fluxes were calculated. These radiative fluxes were then used in the energy equations, and the process was iterated until convergence.

MATLAB was used in the solution. MATLAB is a programming environment for technical computing and modeling (http://www.mathworks.com).

The inputs to the program included solar flux, wind speed, atmospheric pressure, atmospheric temperature, cooling coil temperature, coil leaving air temperature (just after the cooling coils), thickness of exterior wall, thickness of insulation, solar absorptivity of exterior surfaces, and the infrared emissivities of the exterior surfaces, interior surfaces, cooling coils, and the air filter.

Each RTU surface was modeled as one of possible five surface types:

Type 1: A surface with both sides exposed to radiation and convection with conduction through the wall. There are two cases of Type 1 surface. Type 1a has one exterior surface and one interior surface, and Type 1b has two interior surfaces.
Type 2: An adiabatic surface with one side exposed to radiation and convection.
Type 3: A surface subject to radiation on both sides and through which the conditioned air flows.
Type 4: A surface subject to radiation on one side and through which the conditioned air flows.
Type 5: An isothermal surface through which the conditioned air flows.

Figure 4 shows the location of each surface type on the RTU model (see also Figures 2a and 2b for air flow path).

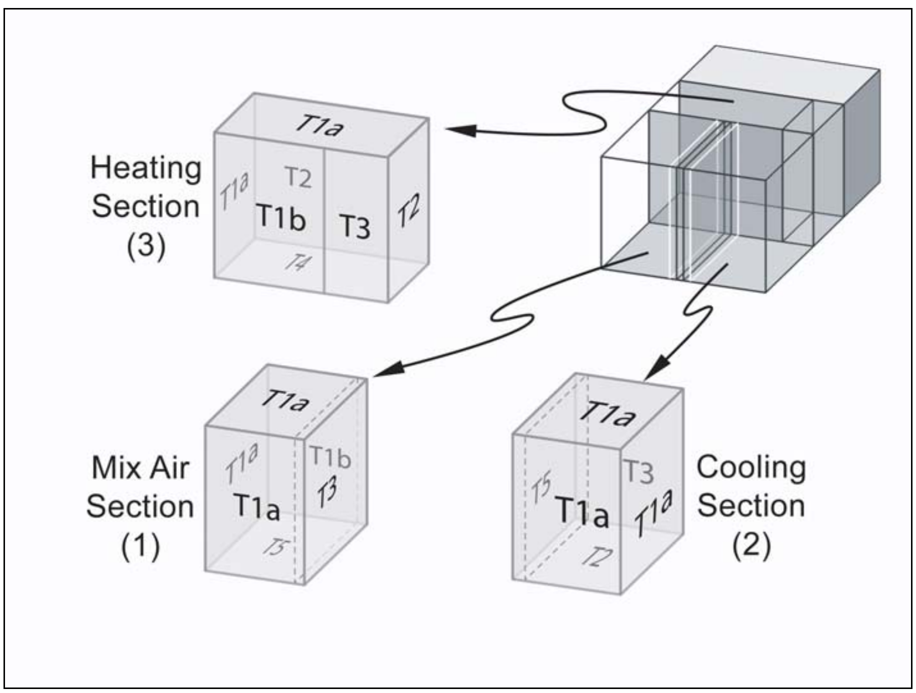

Figure 4: RTU Model Surface Type Location

In the Mix Air Section, the south, west, and top surfaces are of Type 1a, the north surface is of Type 1b, the bottom surface (return air location) is of Type 5, and the east surface is the air filter and is of Type 3. In the Cooling Section, the south, east, and top surfaces are of Type 1a, the bottom surface is of Type 2, the west surface is the cooling coils and is of Type 5, and the north surface is of Type 3.

In the Heating Section, the west and top surfaces are of Type 1a, the north and east surfaces are of Type 2, and the bottom surface (supply air location) is of Type 4. The south surface is split into two portions: south1 and south2. South1, which is adjacent to the Mix Air Section, is of Type 1b. South2, which adjacent to Cooling Section, is of Type 3. Table 1 summarizes the surface types in the RTU model.

Table 1
RTU Model Surface Type Location Summary

Surface Location	Surface Type					
	Type 1a	Type 1b	Type 2	Type 3	Type 4	Type 5
Mix Air Section						
Top	✓					
South	✓					
West	✓					
North		✓				
East (filter)				✓		
Bottom (return air)						✓
Cooling Section						
Top	✓					
South	✓					
West (coils)						✓
North				✓		
East	✓					
Bottom			✓			
Heating Section						
Top	✓					
South1		✓				
South2				✓		
West	✓					
North			✓			
East			✓			
Bottom (supply air)					✓	

SOLAR RADIATION

The selection of the solar radiation levels used in the modeling was based on solar data from the ASHRAE 1995 Fundamentals Handbook (ASHRAE Handbook) and an analysis of all 16 CEC Climatic Zones (CZ01 thru 16) weather data used with eQUEST/DOE-2 building energy simulation program.

The goal of the solar radiation analysis was to select the time of day and the day of year when the sum of the total solar radiation on all surfaces of the RTU was the greatest. From the ASHRAE solar data, September 21 at 10:00 a.m. or 2:00 p.m. produced the largest sum for a location in the Southern California area (32° north latitude) and the RTU model orientation (see Figures 2a and 2b). Table 2 reproduces the relevant solar data from the ASHRAE Handbook for the applicable orientations in the model.

Table 2
ASHRAE Solar Data

Orientation	Solar Radiation (W/m^2)					
	9:00 am	10:00 am	11:00 am	1:00 pm	2:00 pm	3:00 pm
East	636	485	255	101	91	76
South	331	444	513	513	444	331
West	76	91	101	255	485	636
Horizontal	498	643	737	737	643	498
Sum	1540	1663	1607	1607	1663	1540

Of the 16 CEC Climatic Zones, 50 percent of them have latitude between 32 and 34° north, while nearly two thirds have latitudes between 32 and 36° north. The average of the total horizontal solar radiation for all 16 climate zones for the hours of 10:00 a.m. and 2:00 p.m. on September 21 was 649 W/m^2. This value is essentially the same as the horizontal value from the ASHRAE Handbook.

As a result of the similarity of the CEC Climatic Zones and ASHRAE values and the fact that the RTU model has the Cooling Section with exterior surfaces facing south and east, the values for the total (direct and diffuse) solar radiation used in the modeling were based on the ASHRAE data for 10:00 a.m. on September 21. Table 3 lists the total solar radiation used in the analysis.

Table 3
RTU Total Solar Radiation

RTU Surface Orientation	Total Solar Radiation (W/m^2)
East	500
South	450
West	100
Top	650

WIND SPEED

The analysis of all 16 CEC Climatic Zones produced an averaged wind speed of 5.8 mph for the hours of 10:00 a.m. and 2:00 p.m. on September 21. However, for most of the climate zones values ranged between 4 to 10 mph, with one climatic, zone 14, reaching 18 mph at 2:00 p.m. on September 21.

PARAMETRIC RUNS AND TYPICAL CONDITION

In order to evaluate the impact of HRC materials on the supply air temperature and the cooling performance of the RTU, a series of parametric runs were performed. These runs assessed the influence of wind speed and insulation thickness on the supply air temperature for different emissive values. The investigated wind speeds were: 0 (no wind), 1, 5, 7.5, 10, and 15 mph. For each of this wind speeds, the insulation thickness of the RTU surfaces was varied from 0 inches (no insulation) to 1 inch with intermediate values of 0.25, 0.5, and 0.75 inches. For each of the possible combinations of wind speed and insulation thickness, the emissivity was varied from 0.0 (“white”) to 1.0 (“black”) with intermediate values of 0.2, 0.5, and 0.8.

Based on specification from major RTU manufacturers (e.g., Trane, Carrier, Lennox, etc.), the typical insulation thickness for the various surfaces on the RTU cabinet is 0.5 inches. From the analysis of the 16 CEC climate zones, a typical the wind speed of 5 mph can be assumed. Therefore, a typical condition would have an insulation thickness of 0.5 inches, a wind speed of 5 mph, and solar radiation levels as shown in Table 3 for each of the RTU surfaces.

CALCULATIONS

CONDUCTIVE HEAT FLOW

The conductive heat flow is obtained by using the Fourier’s Law

$$Q_k = C_s \bullet A \bullet (T_o - T_i) \qquad (1)$$

where

- Q_k is the conductive heat flow thru the surface
- C_s is the surface thermal conductance (the reciprocal of the surface thermal resistance – it takes into account the metal surface and the insulation)
- A is the surface area
- T_o is the temperature of the outer side of the surface
- T_i is the temperature of the inner side of the surface

CONVECTIVE HEAT FLOW

The convective heat flow is obtained by using Newton's Law of Cooling

$$Q_c = h \bullet A \bullet (T_s - T_{air}) \tag{2}$$

where

- Q_c is the convective heat flow from the surface
- h is the heat transfer coefficient
- A is the surface area
- T_s is the surface temperature
- T_{air} is the air temperature

The heat transfer coefficient is obtained from the Nusselt number, which is given by:

$$Nu = h \bullet L / k_{air} \tag{3}$$

where

- L is a length scale
- k_{air} is the thermal conductivity of air

The Nusselt number (Nu) is a function of Reynolds (Re) and Prandtl (Pr) numbers. For forced convection flow over a flat plate, the Nu relationship used in the analysis is:

$$Nu = 0.0296 \bullet Re^{0.8} \bullet Pr^{0.6}, \text{ for } 0.5 \leq Pr \leq 10 \tag{4}$$

where

- Pr is the Prandtl number of air
- Re is the Reynolds number of the flow

The Reynolds number is defined as:

$$Re = V_{air} \bullet L / \nu_{air} \tag{5}$$

where

- V_{air} is the speed of the air
- L is the characteristic length scale
- ν_{air} is the kinematic viscosity of the air

RADIATIVE HEAT FLOW

The net radiative heat flow leaving an exterior surface of the rooftop unit is given by

$$Q_r = \varepsilon_t \bullet \sigma \bullet (T_s^4 - T_e^4) \bullet A - \alpha_s \bullet q_{solar} \bullet A \tag{6}$$

where

- ε_t is the thermal emissivity of the surface
- is the Stefan-Boltzmann constant
- T_s is the surface temperature
- T_e is the effective radiating temperature of the surrounds (assumed to be the ambient temperature)
- α_s is the solar absorptivity of the surface
- q_{solar} is the solar flux incident on the surface (note the minus sign indicates it is into the surface)
- A is the surface area

The net radiative heat flows leaving the inner surfaces of each section are coupled and are found by solving a linear system of equations where there are as many equations as surfaces. The i^{th} equation can be written as:

$$\sum_{j=1}^{n} [(\delta_{i,j} / \varepsilon_i) - (\rho_j / (\varepsilon_j \bullet A_j)) \bullet A_i \bullet F_{i,j}] \bullet Q_j = \sum_{j=1}^{n} [A_i \bullet F_{i,j} \bullet (B_i - B_j)] \tag{7}$$

where

- $\delta_{i,j} = 1$ if $i = j$ and $\delta_{i,j} = 0$ otherwise
- ε_i is the emissivity of surface i
- ρ_j is the reflectivity of surface j
- ε_j is the emissivity of surface j
- A_i is the area of surface i
- A_j is the area of surface j
- Q_j is the net radiative heat flow leaving surface j
- $F_{i,j}$ is the geometric shape factor between surfaces i and j
- B_i and B_j are the blackbody radiosities of surfaces i and j, respectively

The blackbody radiosity B for a surface at a temperature T is given by:

$$B = \sigma \bullet T^4 \tag{8}$$

The n equations given by Equation (7) can be readily solved when the surface temperatures are known.

The shape factors were obtained from relations given by Edwards (*Edwards, D. K., Radiation Heat Transfer Notes, Hemisphere Publishing Corporation, 1981*) for opposite rectangles and adjacent rectangles. Additionally, shape factor algebra considering offset rectangles was used for the Heating Section.

ENERGY BALANCE

The energy balance for each of the surface types used in the analysis is provided below.

Type 1 Surface

An energy balance on the inner side of a Type 1 surface is given by:

$$h_i \bullet A \bullet (T_i - T_{i,air}) + Q_{r,i} = C_s \bullet (T_o - T_i) \tag{9}$$

and an energy balance on outer side of Type 1 surface is given by:

$$h_o \bullet A \bullet (T_o - T_{o,air}) + Q_{r,o} = C_s \bullet (T_i - T_o) \tag{10}$$

where

- h_{in} is the convective heat transfer coefficient on the inner side of the surface
- h_{out} is the convective heat transfer coefficient on the outer side of the surface
- A is the surface area
- T_i is the temperature of the inner side of the surface
- T_o is the temperature of the outer side of the surface
- $T_{i,air}$ is the air temperature on the inner side of the surface
- $T_{o,air}$ is the air temperature on the outer side of the surface
- C_s is the surface thermal conductance (the reciprocal of the surface thermal resistance)
- $Q_{r,in}$ is the net radiative heat flow (the radiosity minus the irradiation) leaving the inner side of surface
- $Q_{r,out}$ is the net radiative heat flow leaving the outer side of surface

These equations balance the sum of the convective and radiative heat flows leaving a surface side with the conductive heat flow through the surface toward that side.

Equations (1) and (2) can be rearranged as:

$$C_s \bullet T_o - (C_s + h_i \bullet A) \bullet T_i = Q_{r,i} – (h_i \bullet A \bullet T_{i,air}) \tag{11}$$

$$C_s \bullet T_i - (C_s + h_o \bullet A) \bullet T_o = Q_{r,o} – (h_o \bullet A \bullet T_{o,air}) \tag{12}$$

When C_s, h_o, h_i, A, $T_{i,air}$, $T_{o,air}$, $Q_{r,i}$, and $Q_{r.o}$ are known, Equations (3) and (4) can be solved for T_i and T_o as they are simply a linear system of two equations with two unknowns. The radiative heat flows $Q_{r,i}$ and $Q_{r,o}$ are not known a priori and are quartic in T_i and T_o, respectively, as well as quartic in other surface temperatures. So in general an iterative solution is required.

Type 2 Surface

The energy balance on the inner side of a Type 2 (adiabatic) surface is given by:

$$h_i \bullet A \bullet (T_i - T_{i,air}) + Q_{r,i} = 0 \tag{13}$$

and it represents a balance of radiative and convective heat flows which must sum to zero on an adiabatic surface. Solving for T_i gives:

$$T_i = T_{i,air} - Q_{r,i} / (h_i \bullet A) \tag{14}$$

Type 3 and Type 4 Surfaces

The energy balance on the inner side of a Type 3 or Type 4 surface is given by:

$$\dot{m}_{air} \bullet c_{p,air} \bullet (T_i - T_{i,air}) + Q_{r,i} = 0 \tag{15}$$

where

- $\dot{m}_{air}$ is the mass flowrate of air through the surface
- $C_{p,air}$ is the specific heat of the air
- T_i is the temperature of the surface and the air assumed to be in thermal equilibrium
- $T_{i,air}$ is the temperature just before crossing the surface
- $Q_{r,i}$ is the net radiative flux leaving the surface

So, effectively any heat gain or loss by the surface due to radiation is realized in the heat gain or loss by the fluid. The energy balance on the corresponding outer side of a Type 3 surface is identical with each “i” subscripts being replaced with an “o” subscript. The convective heat transfer and energy balance in each of the three sections (Mixed Air, Cooling, and Heating) of the RTU model are given below.

Mixed Air Section

In the Mixed Air Section, the air is taken to be a mixture of 85 percent return air and 15 percent outside air. The air is taken to be fully mixed as it enters the section at a temperature T_{mix}. The air proceeds to pick up thermal energy through convection from the section inner surfaces.

The convective heat transfer to the air in the Mixed Air Section is given as:

$$\begin{aligned} Q_{c,air,1} = {} & h_2 \bullet A_2 \bullet (T_2 - T_{mix}) + h_3 \bullet A_3 \bullet (T_3 - T_{mix}) \\ & + h_4 \bullet A_4 \bullet (T_4 - T_{mix}) + h_5 \bullet A_5 * (T_5 - T_{mix}) \\ & - Q_{r1} - Q_{r6} \end{aligned} \tag{16}$$

The subscripts 1 through 6 correspond to the various surfaces in the section: (1) the bottom surface through which the return air flows, (2) the south surface, (3) the west surface, (4) the top surface, (5) the north surface, and (6) the east surface, which is the air filter. Note that the net radiative heat flows from surfaces 1 and 6 were added here because the air is assumed to have picked up all the heat through convection as shown in Equation (15). An energy balance on the air as it moves through the Mixed Air Section gives:

$$\dot{m}_{air} \bullet c_{p,air} \bullet (T_6 - T_{mix}) = Q_{c,air,1} \qquad (17)$$

As the air passes across the east side of the filter there is a slight cooling before exiting due to the radiative heat loss by the filter to the cooling coils as can be seen in Equation (15). The sensible heat loss by the air by convection to the cooling coils is given by:

$$Q_{c,coils} = \dot{m}_{air} \bullet c_{p,air} \bullet (T_{air,bc} - T_{air,ac}) \qquad (18)$$

where

- $T_{air,bc}$ is the temperature of the air just before encountering the cooling coils
- $T_{air,ac}$ is the temperature just after exiting the cooling coils

<u>Cooling Section</u>

The convective heat transfer to the air in the Cooling Section is given by:

$$\begin{aligned} Q_{c,air,2} = {} & h_1 \bullet A_1 \bullet (T_1 - T_{air,ac}) + h_2 \bullet A_2 \bullet (T_2 - T_{air,ac}) \\ & + h_4 \bullet A_4 \bullet (T_4 - T_{air,ac}) + h_6 \bullet A_6 \bullet (T_6 - T_{air,ac}) \\ & - Q_{r5} \end{aligned} \qquad (19)$$

The subscripts 1 through 6 correspond to the various surfaces in the section: (1) the bottom surface, (2) the south surface, (3) the west surface, which is the cooling coils, (4) the top surface, (5) the north surface, which corresponds to the blower in this analysis, and (6) the east surface. Note that the interaction with the cooling coils does not appear in this equation because it has already been explicitly taken into account. The net radiative transfer of the blower surface is assumed to go into air by convection.

An additional increase in the air temperature occurs due to the net radiative heat transfer to the blower from the Heating Section. Although, the blower motor heat and the blower and motor assembly were not explicitly considered, the blower and motor assembly was modeled as if it has been compressed into the north surface of the Cooling Section, which is also part of the south surface of the Heating Section (see Figures 2a and 2b). The net radiative heat transfer to the north surface of the Cooling Section and to the portion of the south surface of the Heating Section was assumed to be completely picked up by the air by convection. The reason for this assumption was that flow is highly turbulent within the blower, so that the air and the blower would reach thermal equilibrium.

An energy balance on the air as it moves through Cooling Section gives:

$$\dot{m}_{air} \cdot c_{p,air} \cdot (T_5 - T_{air.ac}) = Q_{c,air,2} \tag{20}$$

Heating Section
The convective heat transfer to the air in the Heating Section is given by:

$$\begin{aligned} Q_{c,air,3} = {} & h_3 \cdot A_3 \cdot (T_3 - T_2) + h_4 \cdot A_4 \cdot (T_4 - T_2) \\ & + h_5 \cdot A_5 \cdot (T_5 - T_2) + h_6 \cdot A_6 \cdot (T_6 - T_2) \\ & + h_7 \cdot A_7 + (T_7 - T_2) \\ & - Q_{r2} - Q_{r1} \end{aligned} \tag{21}$$

The subscripts 1 through 7 correspond to the various surfaces in the section: (1) the bottom surface, where the air (supply air) exits the unit, (2) the portion of the south surface where the blower is and the air enters the Heating Section, (3) the portion of the south surface with the Mixed Air Section on the opposite side, (4) the west surface, (5) the top surface, (6) the north surface, and (7) the east surface.

The energy balance on the air in Heating Section is given by:

$$\dot{m}_{air} \cdot c_{p,air} \cdot (T_1 - T_2) = Q_{c,air,3} \tag{22}$$

RESULTS

INSULATION DEPENDENCY

The analysis looked at the impact of insulation thickness on the temperature of supply air leaving the RTU. The RTU was modeled with internal surfaces having no insulation, 0.25, 0.50, 0.75, and 1.0 inches of insulation. From manufacturer's (such as Trane, Carrier, and Lennox) specifications, the typical RTU insulation is aluminum foil-faced fiberglass. The model assumed a fiberglass material with a thermal conductivity of 0.031 Btu/hr-ft-°F and an emissivity of one (insulation is covered with dust).

Figure 5 shows a graph of the supply air temperature versus insulation thickness when the outer surface of the RTU has emissivities of 1.0 (black surface), 0.8 (dark color surface), 0.5 (medium color surface), 0.2 (light color surface), and zero (white surface). The color reference in Figure 5 is only meant to be used as a guide. Materials with emissivities values between 0.5 and 0.2 are considered to be highly reflectivity materials. A curve fitting using a fourth order polynomial was added to graph just to help visualize the trend. Table 4 shows the supply air temperatures for the various insulation thicknesses and emissivity values.

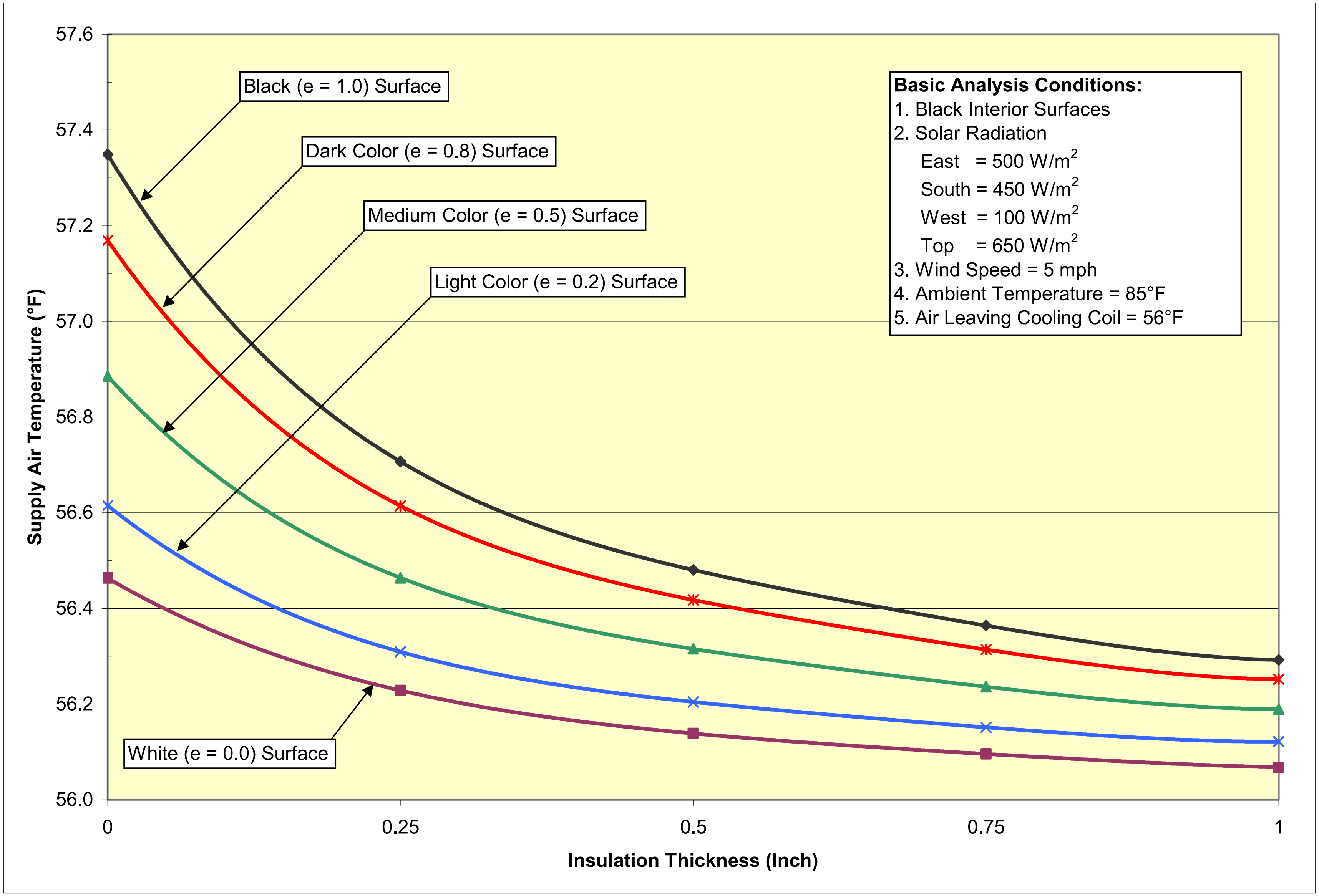

Figure 5: Supply Air Temperature versus RTU Surface Emissivity and Insulation Thickness

Table 4
Supply Air Temperature versus Surface Emissivity and Insulation Thickness

Supply Air Temperature (°F)					
Emissivity	Insulation Thickness (Inch)				
	0.0	0.25	0.5	0.75	1.0
1.0 (“*black*”)	57.35	56.71	56.48	56.36	56.29
0.8 (*“dark”*)	57.17	56.61	56.42	56.31	56.25
0.5 (“*medium”*)	56.89	56.46	56.32	56.24	56.19
0.2 (*“light”*)	56.61	56.31	56.20	56.15	56.12
0.0 (“w*hite”*)	56.46	56.23	56.14	56.10	56.07

EMISSIVITY DEPENDENCY

The analysis looked at the impact of wind speed on the temperature of the supply air leaving the RTU as well as the mixed air entering the cooling coil (Mixed Air Section in the model). The RTU was modeled with 0.5-inch fiberglass insulation, which is typically referenced on manufacturers' specifications.

Figure 6 shows the supply air temperature versus wind speed when the outer surface of the RTU had emissivities of 1.0 (black surface), 0.8 (dark color surface), 0.5 (medium color surface), 0.2 (light color surface), and zero (white surface). Wind speeds of zero, 1, 5, 7.5, 10, 15 mph were modeled. A curve fitting using a third order polynomial was added to graph just to help visualize the trend. Table 5 shows the supply air temperatures for the various wind speed and emissivity values.

Table 5
Supply Air Temperature versus Surface Emissivity and Wind Speed

Supply Air Temperature (°F)						
Emissivity	Wind Speed (mph)					
	0	1	5	7.5	10	15
1.0 (“*black*”)	56.73	56.63	56.48	56.44	56.40	56.36
0.8 (*“dark”*)	56.61	56.53	56.42	56.38	56.35	56.32
0.5 (“*medium”*)	56.44	56.38	56.32	56.29	56.28	56.26
0.2 (*“light”*)	56.24	56.23	56.21	56.20	56.20	56.19
0.0 (“w*hite”*)	56.10	56.12	56.14	56.14	56.15	56.15

Figure 7 shows the mixed air temperature (entering the cooling coil) versus wind speed when the outer surface of the RTU had emissivities of 1.0 (black surface), 0.8 (dark color surface), 0.5 (medium color surface), 0.2 (light color surface), and zero (white surface). Wind speeds of zero, 1, 5, 7.5, 10, 15 mph were modeled. A curve fitting using a third

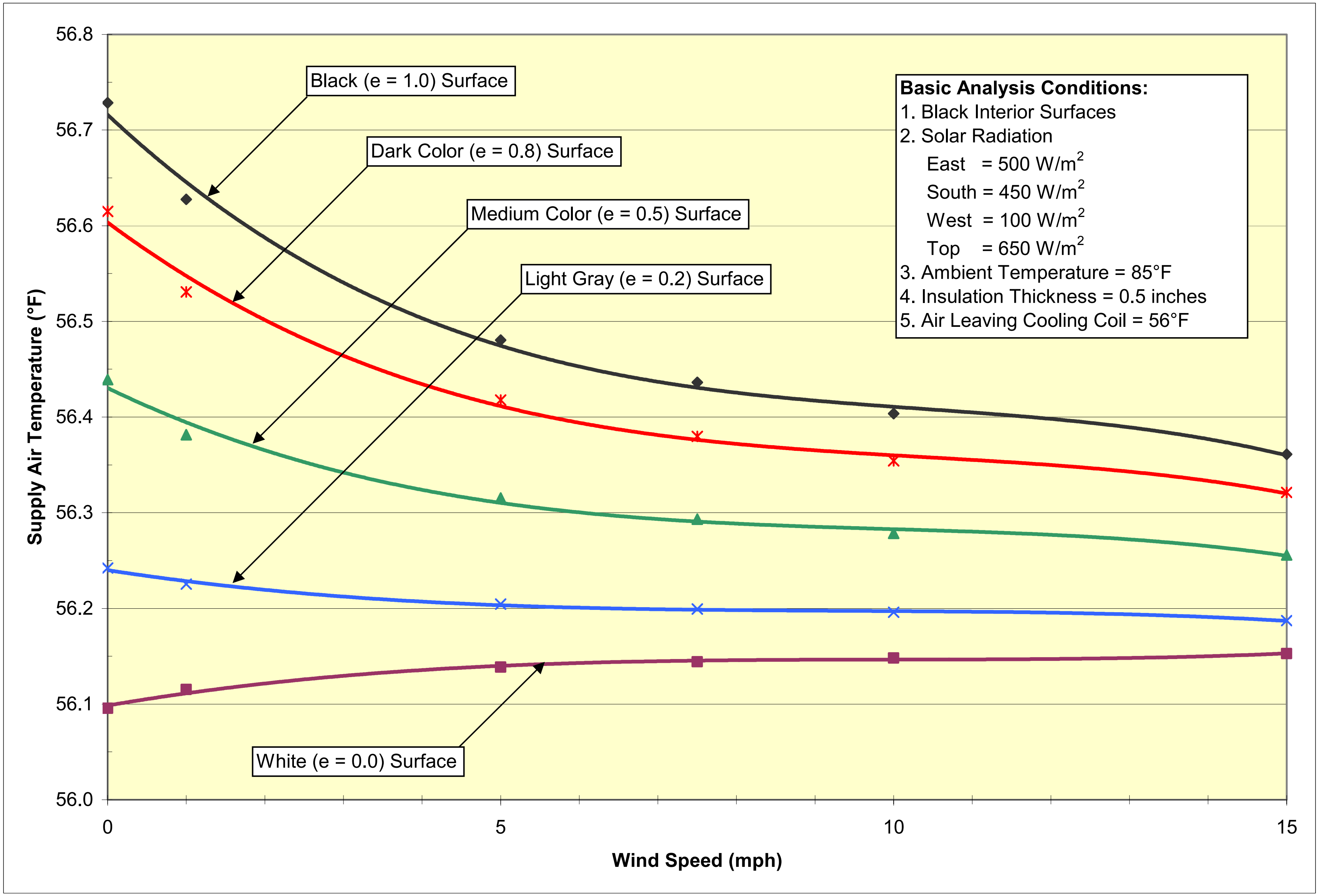

Figure 6: Supply Air Temperature versus RTU Surface Emissivity and Wind Speed

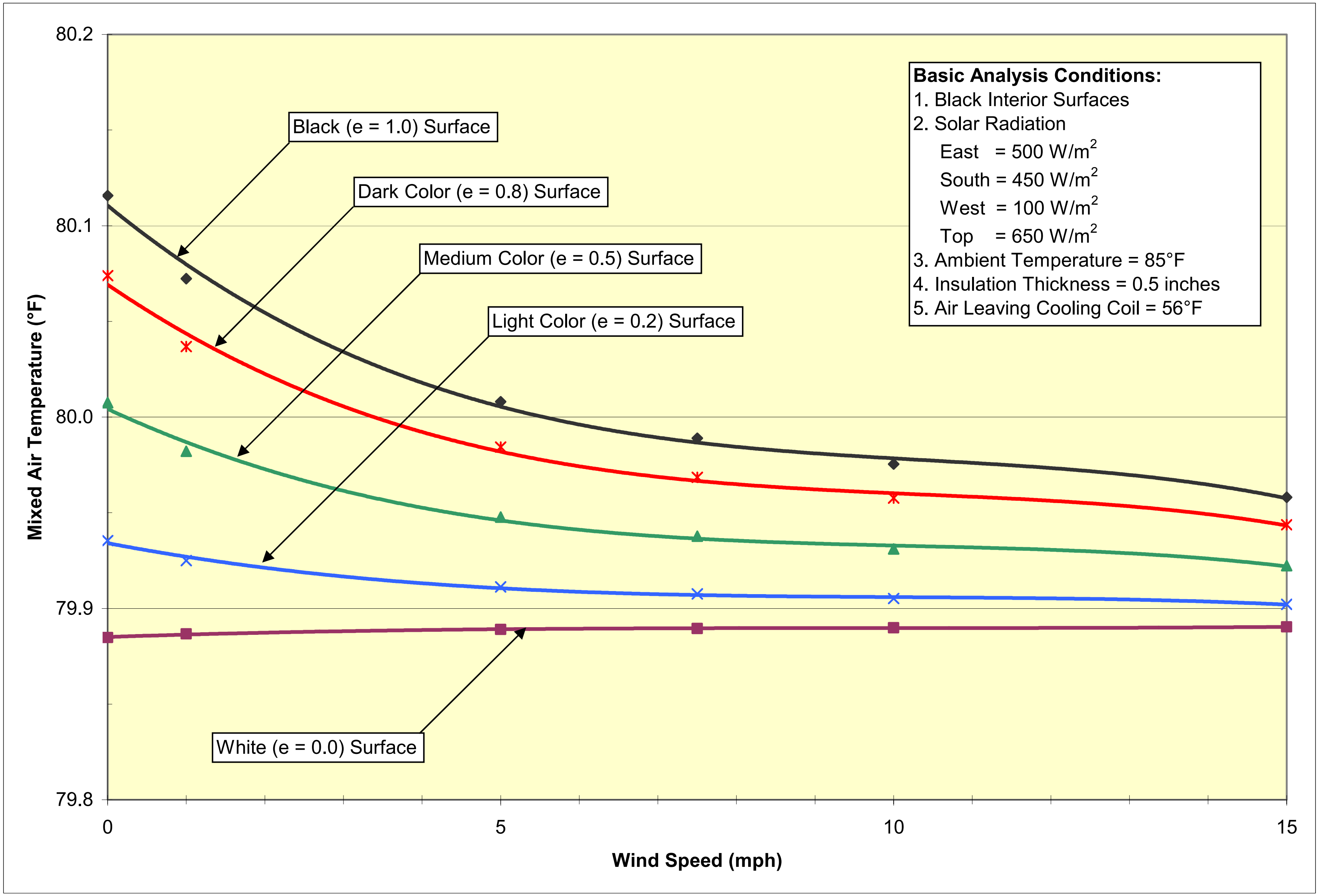

Figure 7: Mixed Air Temperature versus RTU Surface Emissivity and Wind Speed

order polynomial was added to graph just to help visualize the trend. Table 6 shows the mixed air temperatures for the various wind speed and emissivity values.

Table 6
Mixed Air Temperature versus Surface Emissivity and Wind Speed

Mixed Air Temperature (°F)						
Emissivity	Wind Speed (mph)					
	0	1	5	7.5	10	15
1.0 (“*black*”)	80.12	80.07	80.01	79.99	79.98	79.96
0.8 (“*dark*”)	80.07	80.04	79.98	79.97	79.96	79.94
0.5 (“*medium*”)	80.01	79.98	79.95	79.94	79.93	79.92
0.2 (“*light*”)	79.94	79.93	79.91	79.91	79.91	79.90
0.0 (“*white*”)	79.88	79.89	79.89	79.89	79.89	79.89

The color reference in Figures 5, 6 and 7 and Tables 4, 5 and 6 is only meant to be used as a guide. Materials with emissivities values between 0.5 and 0.2 are considered to be highly reflectivity materials.

DISCUSSION

IMPACT OF INSULATION THICKNESS

The results of the analysis show that the supply air temperature rise has a strong dependency on the RTU inner surface insulation thickness. For a RTU with no insulation the supply air temperature went from 56.0°F to 57.17°F when the outer surface has an emissivity of 0.8 (“dark” surface), while the temperature went up to 56.61 when the surface has an emissivity of 0.2 (or reflectivity of 0.8, which represents highly reflective material).

However, for the typical insulation thickness of 0.5 inches, the supply air temperature went up to only 56.42°F when the surface emissivity was 0.8, while the supply air temperature rose to 56.20°F when the surface emissivity was 0.2 (see Figure 5). When the insulation was increase to 1 inch, the difference in the supply air temperature when the surface had an emissivity of 0.8 and 0.2 was about a tenth of a degree (see Table 4 for details).

IMPACT OF WIND SPEED

As shown in Figures 6 and 7, the wind speed has a significant impact of the supply air temperature as well as the mixed air temperature. With no wind, the supply air temperature went from 56.0°F to 56.61°F when the outer surface has an emissivity of 0.8, while the temperature went up to 56.24°F when the surface has an emissivity of 0.2.

However, as in the case of the insulation thickness, with a more typical wind speed of 5 mph, the supply air temperature went up to only 56.42°F when the surface emissivity was 0.8, while the supply air temperature rose to 56.21°F when the surface emissivity was 0.2 (see Figure 6). When the wind speed was increase to 15 mph, the difference in the supply air temperature when the surface had an emissivity of 0.8 and 0.2 was about a tenth of a degree (see Table 5 for details).

The analysis produced similar behavior for the mixed air temperature entering the cooling coil. With no wind, the mixed air temperature went from 79.9°F to 80.07°F when the outer surface has an emissivity of 0.8, while the temperature went up to 79.94°F when the surface has an emissivity of 0.2.

However, with a more typical wind speed of 5 mph, the mixed air temperature rose to 79.98°F when the surface emissivity was 0.8, while the mixed air temperature increased to 79.91°F when the surface emissivity was 0.2 (see Figure 7). When the wind speed was increase to 15 mph, the difference in the mixed air temperature when the surface had an emissivity of 0.8 and 0.2 was four hundreds of a degree (see Table 6 for details).

For the typical case where wind speed is 5 mph and insulation thickness is 0.5 inches, mixed air temperature was 79.98°F when the surface emissivity was 0.8, while the mixed air temperature was to 79.91°F when the surface emissivity was 0.2. Since the coil-leaving air temperature was assumed constant at 56°F, the temperature difference across the cooling coil was 23.98°F and 23.91°F when the surface emissivities were 0.8 and 0.2, respectively. This resulted in an increase of cooling capacity of 0.29 percent (0.07/23.98) due to the HRC material.

Limitations of the Analysis

The modeling of the convective heat transfer within each the three sections (Mixed Air, Cooling, and Heating) of the RTU was based on turbulent flow over a flat plate. Although the geometry of the unit supports this assumption, the actual flow pattern was not investigated for this analysis.

The analysis assumed that air leaving the cooling coil is always at 56°F and that the coil surface is always at 45°F. These assumptions hold reasonably well as long as the outside air temperature is close to 85°F and the air entering the cooling coil is around 80°F. Both of these conditions were maintained in the analysis.

A more dynamic solar radiation might be implemented where hourly fluxes in each of the RTU exterior surfaces are calculated for the entire year. This could be accomplished by using the eQUEST/DOE-2 building energy simulation program weather files.

Although the model was developed based on engineering principals, no validation of the model against field or laboratory data was performed.

CONCLUSION

The analysis shows that a HRC material has the potential to impact the supply air temperature and the RTU cooling performance. Under typical conditions, highly reflective (low emissivity, ε = 0.2) surfaces produced a reduction in supply air temperature (air leaving the unit) of 0.21°F when compared to a low reflectivity (high emissivity, ε = 0.8) surface. This impact could result in the space temperature reaching setpoint sooner and thus the overall compressor run time would be reduced, which, in turn, would result in energy savings.

Also, under the typical conditions, the highly reflective surface (low emissivity, ε = 0.2) produced a reduction in the mixed air temperature of 0.07°F when compared to a low reflectivity surface (high emissivity, ε = 0.8), which resulted in a lower coil-entering air temperature. This lower coil-entering temperature increased the RTU cooling capacity by 0.29 percent. The higher cooling capacity would also reduce the overall compressor run time thus resulting in energy savings.

It is important to emphasize the dependency of the reflective coating impact on a series of factors that were not thoroughly explored in the analysis such as: a) RTU operation (refrigerant charge, air flow, condenser conditions, etc.), b) RTU design (cooling coil arrangement, number of cooling coil rows, use of thermal expansion valve, etc.), c) RTU sizing (under or over sized unit), d) RTU orientation (north, south, etc.), and e) environmental conditions (cooler days, shading). These factors, and in particular, a combination of these factors, may negate or reinforce the impact of the HRC coating material, and will almost certainly add to any uncertainties in the results of the analysis presented in this report.